Accelerated Achilles tendon healing by PDGF gene delivery with mesoporous silica nanoparticles

Arnaud Suwalski, Hinda Dabboue, Anthony Delalande, Sabine F. Bensamoun, Francis Canon, Patrick Midoux, Gerard Saillant, David Klatzmann, Jean-Paul Salvetat, Chantal Pichon

▶ **To cite this version:**

Arnaud Suwalski, Hinda Dabboue, Anthony Delalande, Sabine F. Bensamoun, Francis Canon, et al.. Accelerated Achilles tendon healing by PDGF gene delivery with mesoporous silica nanoparticles. Biomaterials, 2010, 31 (19), pp.5237-5245. ⟨10.1016/j.biomaterials.2010.02.077⟩. ⟨hal-00529475⟩

HAL Id: hal-00529475

https://hal.science/hal-00529475v1

Submitted on 31 Oct 2022

HAL is a multi-disciplinary open access archive for the deposit and dissemination of scientific research documents, whether they are published or not. The documents may come from teaching and research institutions in France or abroad, or from public or private research centers.

L'archive ouverte pluridisciplinaire **HAL**, est destinée au dépôt et à la diffusion de documents scientifiques de niveau recherche, publiés ou non, émanant des établissements d'enseignement et de recherche français ou étrangers, des laboratoires publics ou privés.

HAL Authorization

Accelerated Achilles tendon healing by PDGF gene delivery with mesoporous silica nanoparticles

Arnaud Suwalski*[a], Hinda Dabboue*[b], Anthony Delalande[a], Sabine Bensamoun[c], Francis Canon[c], Patrick Midoux[a], Gérard Saillant[d], David Klatzmann[d], Jean-Paul Salvetat[b,e] and Chantal Pichon[a, §]

[a] Centre de Biophysique Moléculaire, CNRS UPR4301, Université d'Orléans and Inserm, rue Charles Sadron 45071 Orléans Cedex 2, France

[b] Centre de Recherche sur la Matière Divisée, CNRS UMR6619 and Université d'Orléans, 45071 Orléans Cedex 2, France

[c] Laboratoire de BioMécanique et BioIngénierie, CNRS UMR6600, Centre de Recherche de Royallieu – G311 Université Technologique de Compiègne BP 20529, 60205 Compiègne Cedex, France

[d] Laboratoire de biologie et thérapeutique des pathologies immunitaires (Université Pierre et Marie Curie/CNRS UMR 7087), Hôpital de la Pitié-Salpêtrière, 83 Bd de l'hôpital, 75013 Paris, France

[§] Corresponding author: chantal.pichon@cnrs-orleans.fr

Fax number: +33 2 38 63 15 17

Abstract

We report the ability of amino- and carboxyl-modified MCM-41 mesoporous silica nanoparticles (MSN) to deliver gene *in vivo* in rat Achilles tendons. Despite their inefficiency to transfect cells in culture, we show that the luciferase activity lasted for at least 2 weeks in tendons injected with these MSN and a plasmid DNA (pDNA) encoding the luciferase reporter gene. By contrast, in tendons injected with naked plasmid, the luciferase expression decreased as a function of time and became hardly detectable after 2 weeks. Interestingly, there were neither signs of inflammation nor necrosis in tendon, kidney, heart and liver of rat weekly injected with pDNA/MSN formulation during 1.5 months. Our outstanding data concern the acceleration of Achilles tendons healing by PDGF-B gene transfer using MSN. Biomechanical properties and histological analyses clearly indicate that PDGF gene vectorized by MSN treated-tendons healed significantly faster than untreated tendons and those treated with pPDGF alone.

Key words:

silica nanoparticle, MCM-41; gene therapy; growth factor; tendon; non viral gene delivery

1. Introduction

Tendons have a crucial role in maintaining the body mechanics, as their main function is to connect muscles to bones. They are axial connective tissues that ensure transmission of the traction exerted by muscle to bone resulting in joint movements. Tendons are composed of a few cells and parallel arrays of collagen fibers. Their important mechanical function renders them liable to injury and rupture. In human, Achilles tendon is submitted to forces greater than 6-fold the bodyweight. Consequently, Achilles tendon injuries are one of the most common tendon disorders and concern a great part of population. They can be caused by different origins such as overuse that often occurs in sports, consequence of metabolic disease (gut) or age-related loss of elasticity. Tendon heals spontaneously but its regeneration is very difficult and requires a very long period - several months, even a year - which is physically disabling. Moreover, the return at the initial state of the biomechanical parameters is never reached.

Tendon regeneration proceeds in three stages: an inflammatory phase, a cell proliferation phase and a remodelling phase [1, 2]. The inflammatory phase that occurs during the first days after the injury is characterized by fibrin clot formation followed by a mobilization of polymorphonuclear leucocytes as well as other cells involved in the inflammation process. These cells play a part in the cellular debris elimination and secretion of growth factors capable of promoting angiogenesis and tenocytes proliferation. During the proliferation phase, the revascularisation is set up and fibroblasts proliferation makes possible the production of extracellular matrix necessary to fill holes induced by lesions. The remodelling phase can last several months up to years. It is characterized by the reduction in the number of cells and a realignment of the matrix to allow a better response to tensions which the tissue can

undergo. Unfortunately, healed tendons have altered biomechanical properties because of an increase of the water content and a decrease of the quantity and quality of collagen. So later, ruptures can occur and sometimes, a reduction in traction force (loading capacity) is observed due to the tendon tendency to form adherences [3, 4]. These last years, surgery which consists in performing autografts has been improved. However, non-invasive strategies that allow an acceleration of tendon tissues healing are still of interest and remain to be explored.

The mechanism of tendon remodelling and especially the molecular actors that govern its induction and its regulation are known [5]. The process is strongly controlled by growth factors such as bFGF, PDGF (Platelet Derived Growth Factor) and IGF-1 acting at distinct phases of regeneration [6-8]. Indeed, PDGF-BB has a mitogenic activity on fibroblasts and stimulates the collagen I synthesis making it a factor of choice to enhance tendon healing. For instance, a treatment of injured Achilles tendons with PDGF-BB recombinant protein had induced a clear improvement of their regeneration [9]. However, the chronic character of these pathologies requires repeated injections of a large quantity of expensive recombinant. Moreover, the short lifespan of these molecules makes that only a small quantity is delivered on the target and a large one is disseminated in an uncontrolled way causing adverse effects. Thus, the development of alternative methods that will permit a high *in situ* production of these active molecules, such as gene delivery, is strongly desirable.

Different systems including viral or synthetic vectors can be used to deliver genes into the cells. Viral vectors are the most efficient but still remain less safe than synthetic ones, immunogenic and expensive to produce [10]. These last years, cationic lipids [11], polymers [12], carbon nanotubes [13] and silica nanospheres [14]

that form electrostatic complexes with a plasmid DNA (pDNA) have been extensively exploited as chemical vectors for delivering genes. Several studies have reported the use of nanoparticles as drug or gene delivery systems with a low toxicity, improved body distribution, high biocompatibility and improved efficacy [14-18].

MCM-41 mesoporous silicas are inorganic materials that have a porous structure with hundreds of empty channels (mesopores) able to adsorb or encapsulate relatively large amounts of bioactive molecules. They have high surface area (> 900 m^2/g), a large pore volume (> 0.9 cm^3/g) and pore size around 2 to 6 nm. Mesoporous silica nanoparticles (MSN) have been used as *in vitro* DNA vectors [14].

Here, we have used MSN to transfect *in vivo* rat Achilles tendon. For this purpose, MSN surface was modified with amino or carboxyl groups. The novelty of our study concerns the remarkable *in vivo* improvement of tendon regeneration upon the transfer of gene encoding PDGF-B by these silica nanoparticles.

2. Experimental Procedures

2.1 Materials

3-aminopropyltriethoxysilane (APTES, 99 %, Sigma-Aldrich, Saint Quentin Fallavier, France), toluene (for HPLC, 99.8 %, Carlo Erba, Val de reuil, France), succinic anhydride (99 %, Aldrich), anhydrous dimethylsulfoxide (DMSO, Sigma-Aldrich) and absolute ethanol (99.7 %, Carlo Erba) were used as received. *p*-formaldehyde, glutaraldehyde, potassium hexacyanoferrate (III) and lead citrate were obtained from Sigma. Osmiun tetroxide was purchased from Electron Microscopy Sciences (Hatfield, USA).

2.2 Plasmids

pNFCMV-luc was a homemade plasmid DNA of 7.5 kb that encodes the firefly luciferase gene under control of the strong cytomegalovirus (CMV) promoter. Five consecutive κB motifs (termed NF) that recognize the NFκB transcription factor have been inserted upstream of the promoter. pPDGF plasmid (pBLAST-PDGF-B, Invitrogen, Cergy Pontoise, France) encodes the human PDGF-B gene under the ubiquitous EF1 strong promoter. Note that human and rat PDGF-B share more than 90 % of identity. Super coiled pDNA was isolated from bacteria by the standard alkaline lysis method, and purification was carried out with the QIAGEN Mega Kit (QIAGEN, Courtaboeuf, France).

2.3 Surface Modification of Mesoporous Silica Nanoparticles

MCM-41 type MSN was synthesized as described by Lelong *et al.* [19]. The silica surface was substituted with amino groups by reaction at room temperature for 12 h of 73 mg of MSN with 2.5 mL of 3-aminopropyltriethoxysilane (APTES) in anhydrous toluene. Then, amine-functionalized mesoporous silica materials (MSN-NH_2) were filtered, washed with toluene and dried at 60°C for 12 h under vacuum. MSN-COOH particles were prepared as follows. Firstly, 40 mg of MSN-NH_2 were added to 20 mL of toluene and the solution was kept at 50°C until solubilisation. Then, 150 mg of succinic anhydride was allowed to react overnight at room temperature. MSN-COOH particles were separated from the reaction medium by filtration, washed several times with toluene and ethanol and then vacuum-dried. The different MSN were characterized by Fourier transform infrared (FTIR) and zeta potential measurements.

2.4 FTIR experiment

FTIR spectra were collected on a Nicolet 710 FT-IR spectrophotometer with a resolution of 8 cm^{-1} by using the KBr method.

2.5 Zeta potential measurement

Measurements were carried out by electrophoretic mobility using a Zeta Sizer 3000 (Malvern Instruments, Orsay, France). The system was calibrated with the DTS 5050 standard beads from Malvern. Measurements were done 5 times with the zero field correction and performed in 10 mM Hepes buffer, pH 7.4, with the following parameters: viscosity, 0.891 cP, dielectric constant, 79, temperature, 25^{o}C, F(Ka), 1.50 (Smoluchowsky), maximum voltage was 15 V. The zeta potential was calculated using the Smoluchowsky approximation; model Z (Malvern Instrument, Worcestershire, England).

2.6 pDNA/MSN formulations

MSN nanoparticles at 10 mg/ml in distilled water were sonicated for 30 min before use. They were then added to 150 mM NaCl aqueous solution containing pDNA, and the mixture was kept for 30 min at room temperature before transfection. pDNA/MSN formulations (50 µl final volume) were prepared at different weight ratios (µg/µg) from 2:0.6 to 2:5. Formulations were freshly prepared before use.

2.7 Transmission Electron Microscopy analysis

pDNA/MSN formulations were dropped onto the 400 mesh carbon surface of electron microscopy copper grids. After 2 min, the grids were stained for 1 min with 5 % uranyl

acetate and 0.4 % lead citrate and blotted dry. Samples were analysed using a transmission microscope CM20 (Philips) at 200 kV operating voltage.

2.8 Atomic force microscopy (AFM)

The morphology of the pDNA/MSN was analysed by atomic force microscopy (Molecular Imaging Pico +). The samples were prepared by mixing 0.1 µg of pDNA with various amounts of MSN. After 30 min incubation, samples were dropped on freshly cleaved mica surface and allowed to interact for 5 min and then blotted dry.

2.9 Agarose gel electrophoresis

MSN were mixed with pDNA at indicated weight ratio in 50 µl of 10 mM Hepes, pH 7.4. pDNA/MSN or pDNA alone were run on 0.8 % agarose gel containing 0.6 % ethidium bromide for 3 hours at 80 V. Images were taken using a UV transilluminator (Geneflash, Syngene Bio Imaging).

2.10 Primary culture of tenocytes

Tenocytes were obtained from adult Achilles tendon explants. Adult Wistar rats (average weight of 250 g, from Etablissement Dupré (Saint-Doulchard, France) were sacrificed and their tendons were harvested and cut in small pieces in Hank's Buffered Salt Solution pH 7.5 (HBSS). Then, small tendon pieces were placed in tenocytes' medium (DMEM 1 % glutamate, 10 % Fetal Calf Serum, 50 mg/l ascorbic acid, 250 U/ml penicillin, 250 U/ml streptomycin, 0.2 % fungizone) and cultured at 37°C under humidified atmosphere containing 5 % CO_2. After 10 days, first primary cells sprout out from the explants. They were harvested with trypsin, reseeded in 75

cm^2 flask and maintained in tenocytes' medium. Half of the medium volume was replaced every two days.

2.11 *In vitro* transfection

Two days before experiment, tenocytes were seeded at 2 x 10^5 cells on 2 cm^2 well. Then, tenocytes were transfected with 2.5 µg pNFCMV-luc mixed with MSN as described above. After 4 hours, the medium was removed and cells were cultured for two days in tenocytes' medium. The transfection efficiency was determined by measuring the luciferase activity in cell lysates as follows. The culture medium was removed and cells were lysed on ice during 10 min in lysis buffer (1 % Triton X-100, 25 mM Tris-phosphate, 1 mM DTT, 1 mM EDTA, 15 % glycerol, 1 M $MgCl_2$, pH 7.8). *In vitro* luciferase substrate (beetle luciferin, Promega, Madison USA) was added to lysate supernatant in the presence of 1 mM ATP. The Relative Light Units (RLU) produced was measured with a luminometer (Lumat LB9507, Berthold, Thoiry France) and expressed as RLU per mg of proteins upon protein quantification using the BCA colorimetric assay.

2.12 *In vivo* transfection

Adult Wistar rats were stored in CBM's animal house at 22°C and feed *ad libitum* for at least one week before experiments. Rats were anesthetized either with a mixture of ketamine (50 mg/kg) and xylazine (10 mg/kg) in 0.9 % NaCl by intraperitoneal injection or by isoflurane gaz system (AErrane, Baxter, Maurepas, France). Rats' posterior legs were washed with Vetedine© (Centravet, Alfort, France) and shaved. Skin was incised on few millimeters in Achilles tendon region with a carbon steel surgical blade n°11 (Swann-Morton). Achilles tendon was then harmed along its total

length three times using a carbon steel surgical blade n°12 (Swann-Morton). Fifty microliters of pDNA/MSN at a weight ratio of 2:5 were slowly injected in the middle section of Achilles tendon using a Hamilton PBS600 repeater delivery system (5 µl dose per injection). Finally, skin was sutured and rats were closely observed until their wake up. After surgery, animals were treated with subcutaneous injection of fynadine (250 µl/kg) to relieve animals' pain.

The transfection efficiency of pNFCMV-luc treated rats was determined by measuring the luciferase activity in tendon as follows. Rats were euthanized by lethal CO_2 inhalation at day 1, 4, 6, 10 and 15 after surgery. Achilles tendons were harvested and maintained in PBS on ice. Tendons were crushed in liquid nitrogen with mortar and pestle. The powder was added in ice cold lysis buffer (luciferase Cell Culture Lysis, Promega, Madison USA) and the mixture was kept for 3 hours on ice before luminescence measurement. The Relative Light Units (RLU) was measured with a luminometer after adding luciferase substrate (Luciferase Assay System, Promega, Madison, USA) to tendon lysates and expressed as RLU per mg of proteins.

2.13 *In vivo* toxicity assessment

Experiments were carried out with 5 rats per group. Each group received a weekly injection during 6 weeks. The first group was injected with saline solution (150 mM NaCl), the second one with 50 µg MSN and the third one with 20 µg pDNA mixed with 50 µg MSN. Transfected rats were euthanized by lethal CO_2 inhalation. Liver, spleen, kidneys, tendons, and mesenteric lymph nodes were harvested and fixed in 10 % *p*-formaldehyde at room temperature. Then organs were embedded in paraffin wax (Tissue Tek, Sakura Bayer Diagnostics), sliced in serial sections and stained with HES (hematoxyline eosine safranin) (Tissue Tek) and toxicity analyses were

performed by Novaxia (St Laurent Nouan, France). Each slide was inspected microscopically by a pathologist to search for any evidence of damage such as adhesions, necrosis, cellular infiltration or hypervascularity.

2.14 Biomechanical tests

Control and transfected rats were euthanized by lethal CO_2 inhalation at indicated times. Achilles tendons were harvested and stored in PBS at -20°C before use. They were carefully dissected and cleaned to remove muscle tissues. The tendon extremities were glued with cellulose polyacetate and care was taken to prevent gel spreading over the tendon. Then the tendon was clamped between two metal jaws covered with rubber, and mounted vertically on a conventional mechanical test machine (MTS synergie 400). To strengthen the interface between the sample and the jaw, the tendon was surrounded with a piece of rubber. The tendon was preloaded with a velocity of 0.6 mm/min until the applied force reaches 0.1 N. The length (L0) between both extremities of the tendon was measured and the tendon was preconditioned by a cyclic loading, stretching the tendon to 110 % L0 with a velocity of 0.6 mm/min. After pre-conditioning, specimens were stretched to failure at the same rate and the force to failure was recorded (Max. load). The maximal stress (Max. stress) was measured by the force divided by the tendon surface. In addition the Young's modulus (*E*) was also determined.

After mechanical tests, the tendons were fixed in fresh BOUIN's picroformol solution for up to 48 h. Thereafter, tendons were embedded in paraffin and cross sections of 5 µm thickness were cut and stained with Van Gieson's trichrome. The surface of each tendon was manually evaluated from tendon sections mounted on glass slides and analysed by optical microscope using QWIN Leica software.

2.15 Histological analysis

To assess the healing effect of PDGF-B gene transfer, control and injured tendons were harvested at indicated times. They were fixed in 10 % *p*-formaldehyde solution, paraffin embedded, sliced in serial sections (thickness: 4 µm), mounted on glass slides and counterstained with HES stain. Experiments were carried out and analysed by InCellArt (Nantes, France).

2.16 Statistical analysis

Data were expressed by mean ± SD or SEM as indicated. Statistical differences were analyzed by a unilateral Mann–Whitney *U*-test using XLStat 2007 software, and significance was defined as p-value <0.05.

3. Results

3.1 MSN surface modifications

MCM-41 mesoporous silica nanoparticles (MSN) were functionalised with amino or carboxyl groups as described in Fig. 1. The global charges of MSN and modified MSN were assessed by measuring their zeta potential at different steps of functionalization procedure (Table I). Untreated MSN carried a net negative charge of -38.5 mV due to the ionisation of the surface hydroxyl groups. In contrast, the amine modified ones (MSN-NH_2) had a net positive surface charge of 18 mV as a consequence of the presence of amino groups on their surface. MSN-COOH exhibited a negative zeta potential of -49.6 mV resulting from the carboxyl groups created by reaction of amine groups of MSN-NH_2 with succinic acid molecules.

Silica surface modification was also monitored systematically through the different

stages by FTIR spectroscopy (Fig. 2). The unmodified MSN showed the typical vibration bands of siliceous materials, such as that of asymmetric stretching Si-O-Si at ca. 1085 cm^{-1}, symmetric stretching Si-O-Si at ca. 800 cm^{-1}, and stretching vibrations of Si-OH groups at ca. 960 cm^{-1} (Bands located at 1630 and 3430 cm^{-1} come from adsorbed water). The grafting of APTES in MSN-NH_2 samples was confirmed by the presence of adsorption bands at ca. 2900 cm^{-1} attributed to C-H stretching vibrations from propyl groups, and a broad band near 3300 cm^{-1} due to N-H stretching. After reaction with succinic anhydride, amide II band emerges near 1450 cm^{-1}, and amide I band increases intensity and width of 1650 cm^{-1} peak.

3.2 Interactions between DNA and silica nanoparticles

MSN-NH_2 and MSN-COOH were mixed with a pDNA at various weight ratio and their interactions were investigated by zeta potential measurements and agarose gel electrophoresis. When mixed with pDNA, the global charge of MSN-NH_2 became negative (from +17.9 mV to -33.4 mV). This result suggests that electrostatic interactions occurred between the amino charges of MSN-NH_2 and the phosphate groups of pDNA (Table 1). In the case of MSN-COOH, the zeta potential) in the presence of pDNA remained negative (-35.2 mV. Since, the number of amino groups of MSN-COOH was low compared to MSN-NH_2, pDNA was not expected to interact strongly with MSN *via* electrostatic interactions (Table 1). The interactions were also analysed by agarose gel electrophoresis (**Fig. 3**). Whatever the amount of the two MSN types, the migration of pDNA was not completely retarded indicating that the interaction strength was weak. Only one part of pDNA was completely retarded with both MSN types and the amount increased with the pDNA/MSN weight ratio suggesting the presence of some pDNA/MSN complexes. Note that in the presence of MSN up to 100 µg, MSN/DNA interactions were not improved (not shown). TEM

and AFM observations were performed to assess MSN/DNA association (Fig. 4). TEM micrographs of silica nanoplexes made with the two types of MSN showed that nanoparticles are surrounded by loose strands of DNA. However, TEM and AFM showed that a significant amount of DNA remains unbounded.

According to agarose gel electrophoresis, TEM and AFM observations, pDNA was found to interact weakly with two types of MSN. It seems that the nature of the charge or functional group carried by MSN did not influence their capacity to interact with pDNA. The data suggest that pDNA may enwrap MSN *via* surface adsorption with some strand inserted inside pores. Indeed, MSN has a honeycomb-like structure with mesopores large enough to absorb a high amount of biomolecules [17]. Note that the 3 nm pore size of our MSN is compatible with the diameter of a double stranded DNA molecule.

3.3 *In vitro* transfection efficiency of tenocytes

In vitro transfection efficiency of primary tenocytes was evaluated with a plasmid DNA (pDNA) encoding luciferase reporter gene (p-Luc) in the presence of various amounts of MSN-NH_2 or MSN-COOH nanoparticles and Jet-PEI^{TM} was used as gold standard transfection reagent (Fig. 5). The transfection efficiency with MSN-NH_2 and MSN-COOH at pDNA/MSN weight ratio of 2:5 and 2:10 was very low and similar to that obtained with naked pLuc. Comparatively, the luciferase activity produced with Jet-PEI^{TM} polyplexes was 100-fold higher than with bare pDNA. We found that these two types of MSN/pDNA formulations were also unable to transfect other cell types including human embryonic kidney (HEK293) cells, known to be easily transfected by most of transfection reagents (not shown). This absence of efficacy on cultured cells may be due to the weak interactions of pDNA with both MSN. It is known that pDNA compaction is usually required to avoid its degradation by serum nucleases in culture

medium and to enhance its cellular uptake. Moreover, the negative zeta potential of pDNA/MSN probably did not favour their internalization by the cells. Indeed, when the tenocytes were incubated with MSN formulated with fluorescein-labelled pDNA, flow cytometry analysis showed that there was no difference between the cell-associated fluorescence intensities measured after 4°C and 37°C incubation (not shown). Accordingly with the above data, this result evidenced a very low pDNA uptake by tenocytes, and therefore it is not surprising that transfection was not efficient.

3.4 Achilles tendons transfection

In spite of the absence of transfection of primary tenocytes, we tested the efficiency of these pDNA/MSN upon direct injection in rat Achilles tendons. In the first set of experiments, tendons were transfected with pLuc, and 3 days post-transfection the luciferase activity was evaluated. Surprisingly, the two MSN types were able to transfect efficiently tendons at a pLuc/MSN weight ratio of 2:2.5 (Fig.7)**.** The efficacy at a pLuc/MSN weight ratio of 2:5 was not significantly different (not shown). It is worth to note that similar transfection efficacy was obtained on injured or healthy tendons (not shown). Although MSN-NH_2 was as efficient as MSN-COOH, we decided to use the latter because we thought that anionic silica nanoparticles will be less toxic than the amino ones and would lead to a better clearance. Indeed, it is known that positive charged particles could be stuck within negatively charged extracellular matrix components. Next, dose response experiments were carried out with 2.5, 5, 10 and 20 µg of pLuc formulated with MSN-COOH in tendons. Fig. 6 indicates that the gene expression was dependent on pLuc dose and a plateau was reached at 10 µg pDNA (1.6×10^6 RLU/mg of proteins).

The kinetics of gene expression was performed with 5 µg pDNA (Fig. 7). One day post-transfection, the luciferase activity obtained from lysates of tendons transfected with pLuc/MSN-COOH was high (10^7 RLU/mg of proteins) but not significantly different to that obtained with pLuc alone. Then, this activity decreased the following days but not with the same manner. At day 10 and day 15 post-injection, the luciferase activity in pLuc/MSN-COOH nanoplexes-injected tendons detected was 10 and 100-fold less than that measured at day 3, respectively. Comparatively, in tendons injected with pLuc alone, this activity was 114-fold and 1500-fold lower than that at day 3. Similar differences were also observed when 20 µg pDNA was injected in tendons.

3.5 MSN toxicity

Repeated injections (one per week during 6 weeks) of either free MSN-COOH or pDNA/MSN were done locally in rat Achilles tendons. Rats were checked up every day for close observations, and vital organs (liver, spleen, kidney, mesenteric lymph node and lung) as well as tendons were harvested after 6 weeks for histopathological analyses. As shown in Fig. 8, no histopathology changes in terms of inflammation, necrosis or structural tissue organization were observed in vital organs of treated groups *versus* untreated ones. It is worth to note that no signs of inflammation were observed in tendons after 3 days post-injection.

3.6 Healing activity of PDGF gene transfer

The absence of toxicity upon pDNA/MSN transfection prompted us to evaluate their efficacy to transfer the PDGF-B gene for tendon healing. Rat Achilles tendons were injured and then treated or not with plasmid encoding PDGF gene (pPDGF). For that, 20 µg of pPDGF were used alone or mixed with MSN-COOH. In control rats, healthy tendons were injected with physiological serum or with a plasmid encoding luciferase

gene. The benefit effect of the treatment was assessed by biomechanical tests and tendon histology. In terms of biomechanical properties, parameters defined by maximal load to failure, maximum stress and Young's modulus were significantly greater in pPDGF/MSN or in naked pPDGF-treated groups than in untreated one (Table 2). It is worth to note that there is a high variability of Young's modulus values of injured tendons treated with pPDGF alone (88.79 ± 16.39 MPa) which is not the case of that of tendons treated with pPDGF/MSN. Remarkably, the values of maximal load, maximal stress and Young's modulus of tendons treated with pPDGF/MSN are very close to those of healthy (control) tendons (96.57 ± 7.7 *vs* 96.25 ± 4.19 MPa).

To improve the organization of tendon structure, we treated injured tendon with two injections of pPDGF spaced by one week interval. Histological analyses at 21 days post-injury showed that a faster regenerating activity occurred in treated tendons than in the untreated groups (Fig. 9). This was supported by the following observations: i) a higher number of fibroblasts was observed in untreated tendons than in tendons treated with pPDGF or pPDGF/MSN indicating that untreated tendons were still in proliferative phase after 2 weeks of injury and ii) treated tissues were nicely organized by contrast to those that were mock treated. More importantly, tendons that have been treated with pPDGF/MSN exhibited the highest structural organization with more aligned fibers compared to tendons treated with pPDGF alone.

4 Discussion

Several reports have shown that silica nanoparticles can be used as carrier to deliver gene in vitro [14]. Silica nanoparticles are usually modified by various means to exhibit positive charges providing electrostatic binding with negatively charged DNA. In the present study, we provide evidences that mesoporous silica nanoparticles,

substituted either with amino or carboxyl groups, can be used *in vivo* for gene delivery in rat Achilles tendons despite being inefficient *in vitro* on primary cultures of tenocytes.

Both pDNA/MSN-NH_2 and pDNA/MSN-COOH nanoplexes exhibited a negative zeta potential of about -35 mV at pH=7.4. This suggests that direct electrostatic interaction is not the main driving force for association of pDNA on MSN. It is probable that hydrogen bonding between silanol and phosphate groups plays an important role in pDNA-MSN interaction [20, 21]. Our results could also suggest that segments of pDNA were inserted inside MSN pores. In the case of MSN-NH_2, a propyl group was used as spacer between the surface of MSN and the amino group. This was also the spacer used to prepare ORMOSIL amino silica nanoparticles [22], In this case, pDNA/ORMOSIL interactions were also weak. Indeed, pDNA was not completely retarded under agarose gel electrophoresis. The propyl length may be too short to allow strong electrostatic interactions with pDNA due to screening effects. Indeed, a complete pDNA retardation was obtained at a pDNA/MSN weight ratio of 1:5 (µg:µg) when a hexyl-amino-propyl spacer was used [23] as well as when MSN was capped with polyamidoamine dendrimer [24]. The absence of strong interactions between MSN and pDNA as well as the negative zeta potential of pDNA/MSN explain the absence of efficient transfection of cultured tenocytes as well as other cell lines *in vitro*. This result is coherent with previous reports clearly indicating that for *in vitro* transfection, positive complexes are required to get enhanced interactions with plasma membrane and high enough protection against extracellular degradation. In the case of silica nanoparticles, Kneuer *et al.* [18] have shown that a high weight ratio of silica pDNA/nanoparticles (1:30) was needed to get positive charged nanoplexes efficient for *in vitro* transfection. The use of such large amount of silica nanoparticles

could induce biological side effects (see below) [25]. Of interest, our MSN are able to transfer gene efficiently *in vivo* in tendons. Such behavior has also been found for amphiphilic block copolymers such as Lutrol or Pluronic that are not efficient to transfect cells *in vitro* whereas they show high efficacy to transfect skeletal muscles upon intramuscular injection or lung upon intratracheal instillation [26-28]. In our case, no transfection was observed upon intramuscular injection of pDNA/MSN formulations (data not shown). The probable explanation is that pDNA/MSN were able to diffuse upon injection in tendons allowing the transfection of a large area whilst they stuck at the site of injection and did not diffuse at all upon intramuscular injection (Pichon *et al*., unpublished observations).

Data concerning the kinetics of gene expression reveal the gradual diminution of the luciferase activity that can likely be contributed to the time release behavior of pDNA adsorbed on or entrapped in MSN.

Our outstanding data concerns the acceleration of the regeneration activity by PDGF gene transfer with MSN. Tendons are viscoelastic tissues and therefore their internal organization mainly based on collagen I is crucial [29, 30]. In rat Achilles tenocytes, Wang *et al.* have shown that *in vitro* transfection of PDGF-B gene promotes a positive effect on collagen I production [31]. Note that, the level of luciferase produced in tendons upon transfectionwas close to the active dose of recombinant PDGF-BB (related to the nanogram range). Our data clearly show a fast recovery of biomechanical property of pPDGF/MSN treated tendons which is sustained by a remarkable tissue organization. The structural organization of fibers was aligned along with the functional loading axis in pPDGF/MSN treated groups. By contrast, naked pPDGF treated tendons still exhibited areas of more disorganized collagen, i.e., collagen fibers diverging from the functional axis.

The adverse biological effects of nanomaterials such as silica nanoparticles raise safety concerns on their use. Several reports have assessed the biological side effects that could induce silica nanoparticles. They have shown that silica nanoparticles can induce inflammatory (NFκB activation) and oxidative stress responses both *in vivo* and *in vitro* [32-35] but these effects were only observed at high concentrations [25, 36]. Recent studies have demonstrated by comet assay that silica nanoparticles with size ranging from 20 to 400 nm do not exert significant genotoxicity [25, 36]. The toxicity of our pDNA/MSN was addressed by investigating the chronic effect they could induce. Gross observations of tendon and histological analyses indicated that no local inflammation or necrosis was induced after several injections. Note that no acute inflammatory process was observed after one or 3 days post-injection (not shown). We are, however, conscious that before human application, a battery of standardized tests to quantify genetic aberrations must be performed to cover all potential forms of DNA damage that may be induced following the local injection of silica nanoparticles in Achilles tendons.

Conclusions

Results reported in this study clearly demonstrate that mesoporous silica nanoparticules can be exploited to efficiently deliver genes in Achilles tendons. The delivery of pDNA with MSN allows a sustained gene expression for at least 2 weeks. Our remarkable result concerns the improvement of healing of injured tendons by PDGF gene transfer. Nevertheless, co-transfection with other genes encoding active molecules involved in healing will be addressed to restore a tendon structure as aligned as in healthy tendons.

Acknowledgments

This work was supported by AFM (Association Française contre les Myopathies) and French National Research Agency (ANR) Project Bionanocomp ANR-05-BLAN-0164. Arnaud Suwalski received a PhD fellowship from AFM. The authors would like to acknowledge Fabienne Warmont, Loïc Lebegue and Cristine Gonçalves for their skilful technical help.

References

1. Hildebrand KA, Frank CB, Hart DA. Gene intervention in ligament and tendon: current status, challenges, future directions. Gene Ther 2004 Feb;11(4):368-378.
2. Woo SL, Debski RE, Zeminski J, Abramowitch SD, Saw SS, Fenwick JA. Injury and repair of ligaments and tendons. Annu Rev Biomed Eng 2000;2:83-118.
3. Gelberman RH, Boyer MI, Brodt MD, Winters SC, Silva MJ. The effect of gap formation at the repair site on the strength and excursion of intrasynovial flexor tendons. An experimental study on the early stages of tendon-healing in dogs. J Bone Joint Surg Am 1999 Jul;81(7):975-982.
4. Manske PR. Flexor tendon healing. J Hand Surg Br 1988 Aug;13(3):237-245.
5. Molloy T, Wang Y, Murrell G. The roles of growth factors in tendon and ligament healing. Sports Med 2003;33(5):381-394.
6. Sciore P, Boykiw R, Hart DA. Semiquantitative reverse transcription-polymerase chain reaction analysis of mRNA for growth factors and growth factor receptors from normal and healing rabbit medial collateral ligament tissue. J Orthop Res 1998 Jul;16(4):429-437.
7. Chan BP, Chan KM, Maffulli N, Webb S, Lee KK. Effect of basic fibroblast growth factor. An in vitro study of tendon healing. Clin Orthop Relat Res 1997 Sep(342):239-247.
8. Duffy FJ, Jr., Seiler JG, Gelberman RH, Hergrueter CA. Growth factors and canine flexor tendon healing: initial studies in uninjured and repair models. J Hand Surg Am 1995 Jul;20(4):645-649.
9. Aspenberg P, Virchenko O. Platelet concentrate injection improves Achilles tendon repair in rats. Acta Orthop Scand 2004 Feb;75(1):93-99.
10. Giannoudis PV, Tzioupis CC, Tsiridis E. Gene therapy in orthopaedics. Injury 2006 Apr;37 Suppl 1:S30-40.
11. Montier T, Benvegnu T, Jaffres PA, Yaouanc JJ, Lehn P. Progress in cationic lipid-mediated gene transfection: a series of bio-inspired lipids as an example. Curr Gene Ther 2008 Oct;8(5):296-312.
12. Midoux P, Pichon C, Yaouanc JJ, Jaffres PA. Chemical vectors for gene delivery: a current review on polymers, peptides and lipids containing histidine or imidazole as nucleic acids carriers. Br J Pharmacol 2009 May;157(2):166-178.
13. Son SJ, Bai X, Lee SB. Inorganic hollow nanoparticles and nanotubes in nanomedicine Part 1. Drug/gene delivery applications. Drug Discov Today 2007 Aug;12(15-16):650-656.
14. Slowing, II, Vivero-Escoto JL, Wu CW, Lin VS. Mesoporous silica nanoparticles as controlled release drug delivery and gene transfection carriers. Adv Drug Deliv Rev 2008 Aug 17;60(11):1278-1288.

15. Kim SY, Lee YM, Baik DJ, Kang JS. Toxic characteristics of methoxy poly(ethylene glycol)/poly(epsilon-caprolactone) nanospheres; in vitro and in vivo studies in the normal mice. Biomaterials 2003 Jan;24(1):55-63.
16. Vallet-Regi M. Ordered mesoporous materials in the context of drug delivery systems and bone tissue engineering. Chemistry 2006 Aug 7;12(23):5934-5943.
17. Chung TH, Wu SH, Yao M, Lu CW, Lin YS, Hung Y, et al. The effect of surface charge on the uptake and biological function of mesoporous silica nanoparticles in 3T3-L1 cells and human mesenchymal stem cells. Biomaterials 2007 Jul;28(19):2959-2966.
18. Kneuer C, Sameti M, Bakowsky U, Schiestel T, Schirra H, Schmidt H, et al. A nonviral DNA delivery system based on surface modified silica-nanoparticles can efficiently transfect cells in vitro. Bioconjug Chem 2000 Nov-Dec;11(6):926-932.
19. Lelong G, Bhattacharyya S, Kline S, Cacciaguerra T, Gonzalez MA, Saboungi ML. Effect of surfactant concentration on the morphology and texture of MCM-41 materials. J Phys Chem C 2008 Jul;112(29):10674-10680.
20. Murashov VV, Leszczynski J. Adsorption of the phosphate groups on silica hydroxyls: An ab initio study. Journal of Physical Chemistry A 1999 Mar;103(9):1228-1238.
21. Mao Y, Daniel LN, Whittaker N, Saffiotti U. DNA-Binding To Crystalline Silica Characterized By Fourier-Transform Infrared-Spectroscopy. Oxygen Radicals and Lung Injury Conference; 1993 Aug 30-Sep 02; Morgantown, Wv; 1993. p. 165-171.
22. Roy I, Ohulchanskyy TY, Bharali DJ, Pudavar HE, Mistretta RA, Kaur N, et al. Optical tracking of organically modified silica nanoparticles as DNA carriers: a nonviral, nanomedicine approach for gene delivery. Proc Natl Acad Sci U S A 2005 Jan 11;102(2):279-284.
23. Ravi Kumar MN, Sameti M, Mohapatra SS, Kong X, Lockey RF, Bakowsky U, et al. Cationic silica nanoparticles as gene carriers: synthesis, characterization and transfection efficiency in vitro and in vivo. J Nanosci Nanotechnol 2004 Sep;4(7):876-881.
24. Radu DR, Lai CY, Jeftinija K, Rowe EW, Jeftinija S, Lin VS. A polyamidoamine dendrimer-capped mesoporous silica nanosphere-based gene transfection reagent. J Am Chem Soc 2004 Oct 20;126(41):13216-13217.
25. Chang JS, Chang KL, Hwang DF, Kong ZL. In vitro cytotoxicitiy of silica nanoparticles at high concentrations strongly depends on the metabolic activity type of the cell line. Environ Sci Technol 2007 Mar 15;41(6):2064-2068.
26. Desigaux L, Gourden C, Bello-Roufai M, Richard P, Oudrhiri N, Lehn P, et al. Nonionic amphiphilic block copolymers promote gene transfer to the lung. Hum Gene Ther 2005 Jul;16(7):821-829.
27. Richard P, Bossard F, Desigaux L, Lanctin C, Bello-Roufai M, Pitard B. Amphiphilic block copolymers promote gene delivery in vivo to pathological skeletal muscles. Hum Gene Ther 2005 Nov;16(11):1318-1324.
28. Bello-Roufai M, Lambert O, Pitard B. Relationships between the physicochemical properties of an amphiphilic triblock copolymers/DNA complexes and their intramuscular transfection efficiency. Nucleic Acids Res 2007;35(3):728-739.
29. Oxlund H. Relationships between the biomechanical properties, composition and molecular structure of connective tissues. Connect Tissue Res 1986;15(1-2):65-72.
30. Kirkendall DT, Garrett WE. Function and biomechanics of tendons. Scand J Med Sci Sports 1997 Apr;7(2):62-66.
31. Wang XT, Liu PY, Tang JB. Tendon healing in vitro: genetic modification of tenocytes with exogenous PDGF gene and promotion of collagen gene expression. The Journal of hand surgery 2004 Sep;29(5):884-890.
32. Park EJ, Choi J, Park YK, Park K. Oxidative stress induced by cerium oxide nanoparticles in cultured BEAS-2B cells. Toxicology 2008 Mar 12;245(1-2):90-100.

33. Sayes CM, Reed KL, Warheit DB. Assessing toxicity of fine and nanoparticles: comparing in vitro measurements to in vivo pulmonary toxicity profiles. Toxicol Sci 2007 May;97(1):163-180.
34. Lin W, Huang YW, Zhou XD, Ma Y. In vitro toxicity of silica nanoparticles in human lung cancer cells. Toxicol Appl Pharmacol 2006 Dec 15;217(3):252-259.
35. Kaewamatawong T, Shimada A, Okajima M, Inoue H, Morita T, Inoue K, et al. Acute and subacute pulmonary toxicity of low dose of ultrafine colloidal silica particles in mice after intratracheal instillation. Toxicol Pathol 2006;34(7):958-965.
36. Jin Y, Kannan S, Wu M, Zhao JX. Toxicity of luminescent silica nanoparticles to living cells. Chem Res Toxicol 2007 Aug;20(8):1126-1133.

Figure Captions

Figure 1: Functionalization scheme of MCM-41. APTES: 3-aminopropyltriethoxysilane.

Figure 2: Fourier-transform IR (FTIR) absorbance spectra of MSN and modified MSN.

Figure 3: pDNA/MSN interactions

MSN-COOH and MSN-NH_2 were mixed with pDNA at a pDNA/MSN weight ratio (µg/µg) of 2/0.6 (line 1), 2/1.25 (line 2 & 5), 2/2.5 (lines 3 & 6) and 2/5 (lines 4 & 7). Line C corresponds to pDNA alone. Agarose gel electrophoresis was carried out and DNA was revealed by Ethidium Bromide fluorescence upon DNA intercalation. Arrow: retarded DNA.

Figure 4: TEM and AFM analyses.

A. Representative Transmission Electron microscopy images of naked plasmid DNA (a), MSN-NH2 (b), MSN-COOH (c), pDNA/MSN-NH_2 (d), pDNA/MSN-COOH (e).

B. Intermittent mode AFM images of nanoplexes deposited on mica surface by blotting. Left: DNA/MSN-COOH 2:2.5 Right DNA/MSN-NH2 2:5. Images suggest that most nanoparticles are linked to DNA. When MSN were not mixed to DNA they did not bind to the mica surface, which confirms the attractive interaction between MSN and DNA.

Figure 5: *In vitro* transfection

Tenocytes were transfected with 5 µg of pDNA encoding luciferase gene (pLuc) alone or formulated with MSN-NH_2, MSN-COOH or Jet-PEI™. The luciferase activity (RLU/mg of proteins) was measured two days after transfection.

Figure 6: *In vivo* dose response experiments

Rat Achilles tendon were injected with 2.5, 5, 10 and 20 µg of pDNA encoding luciferase gene mixed with MSN-COOH at weight ratio of 2:5. Rats were killed and tendons were harvested at day 3 post-injection. The luciferase activity (RLU/mg of proteins) was measured as described in Material and Methods. The number of animals per groups was at least n = 4. Values were mean ± SEM.

Figure 7: Kinetics of transgene expression in Achilles tendon.

Rat Achilles tendon were injected with 5 µg of pDNA encoding luciferase gene alone or mixed with 6.25 µg of MSN-COOH. Rats were killed and tendons were harvested at days 1, 3, 6 and 15 post-injection. The luciferase activity (RLU/mg of proteins) was measured as described in Material and Methods. The number of animals per

groups was n = 5. Values were mean ± SEM. * significant difference ($p < 0.05$) between pDNA/MSN-CCOH and pDNA alone

Figure 8: Toxicity assessment.

Shown are representative light micrographs of vital organs of rats treated with or without MSN-COOH/pDNA at weight ratio of 2:5. (A) control kidney, (B) pDNA/MSN-treated kidney, (C) control kidney, (D) pDNA/MSN-treated kidney, (E) control liver (F) pDNA/MSN-treated liver, (G), control tendon and (H) pDNA/MSN-treated tendon. Each group received a weekly injection in tendon during 6 weeks before euthanasia. Vital organs were harvested and processed for histology experiments.

Figure 9: Histological analyses of pDNA/MSN treated Achilles tendons.

Injured Achilles tendons were treated with pPDGF alone or formulated with MSN-COOH. Twenty days post-treatment healthy and treated tendons were harvested, fixed in 10 % *p*-formaldehyde solution, paraffin-embedded, sliced in serial sections (4 µm), mounted on glass slides and HES counterstained. Images shown are representative sections (10 fold magnification) of at least 4 tendons from healthy tendon (A), non-treated tendon (B), pPDGF-treated tendon (C) and pPDGF/MSN-treated tendon (D). The delineated circle corresponds to injury area.

Table I Zeta-potential values of MSN and pDNA/MSN

Zeta potential (mV)		
Materials	**Without pDNA**	**With pDNA**
MSN	-38,5	-
MSN-NH_2	+17,9	-33,4
MSN-COOH	-49,6	-35,2

Zeta potential measurements of amino- or carboxy-modified MCN-41 silica particles before and after mixing with pDNA. All measurements were performed in 10 mM Hepes buffer, pH 7.4.

Table 2: Biomechanical properties

Populations	Maximal load (N)	Maximal stress (MPa)	Young's modulus (MPa)
Control (*n=11*)	31.58 ± 1.89 *	29.60 ± 2.54 *	96.25 ± 4.19 *
pPDGF (*n=8*)	32.52 ± 2.51 *§	31.36 ± 3.84 *§	88.79 ± 16.39 *§
pPDGF/MSN (*n=7*)	34.58 ± 2.79 *§	26.31 ± 3.63 *§	96.57 ± 7.7 *§
Untreated (*n=12*)	24.19 ± 1.96	20.18 ± 2.62	68.15 ± 7.63

Maximal load, maximal stress and Young's modulus obtained with the mechanical tests: control: healthy tendons, pPDGF: injured tendons injected with pPDGF alone, pPDGF/MSN: injured tendons treated with pPDGF/MSN-COOH, Untreated: injured tendons treated with saline. Values are mean ± standard error of the mean (SEM). * Significant statistical difference ($p < 0.05$) compared to untreated group. § No significant statistical difference compared to healthy group.

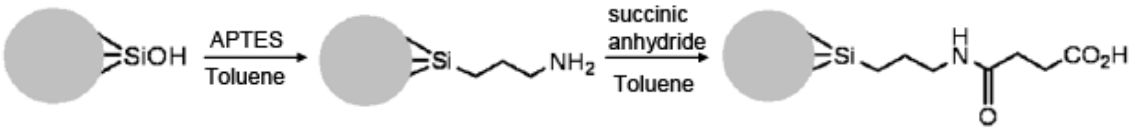
SiOH
APTES
Toluene
Si
NH2
succinic
anhydride
Toluene
Si
H
N
O
CO2H

Figure 1

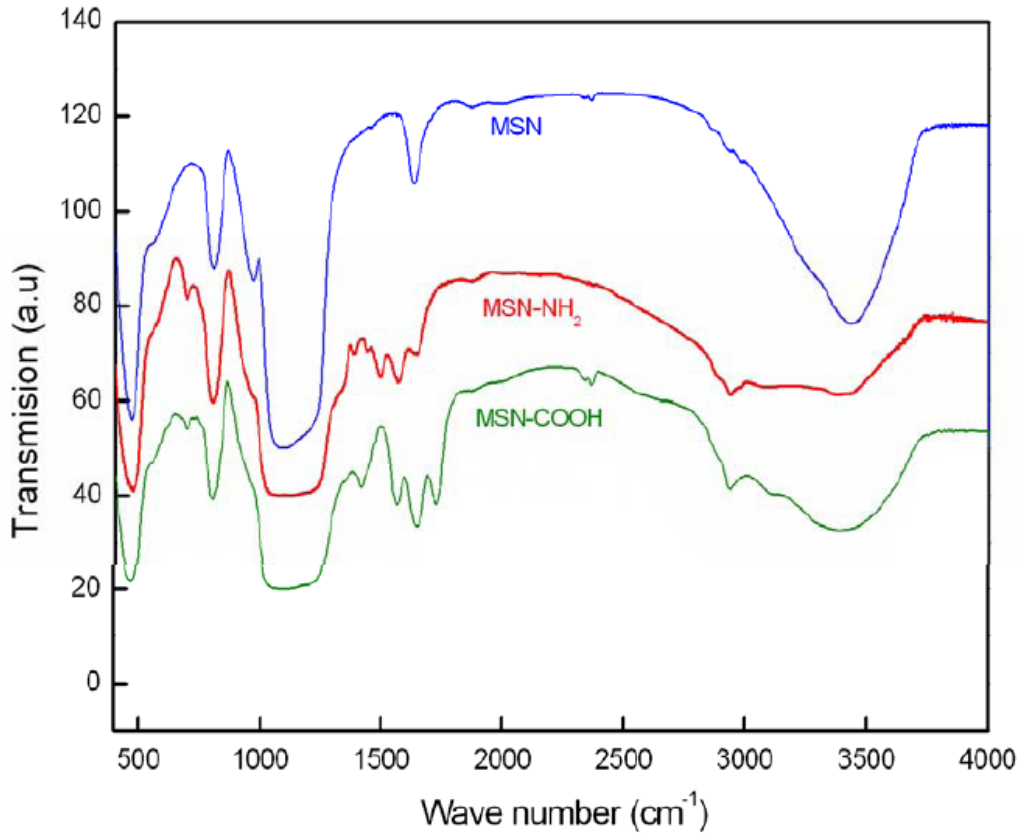
140
120
100
80
60
40
20
0
Transmision (a.u)
MSN
MSN-NH2
MSN-COOH
500
1000
1500
2000
2500
3000
3500
4000
Wave number (cm-1)

Figure 2

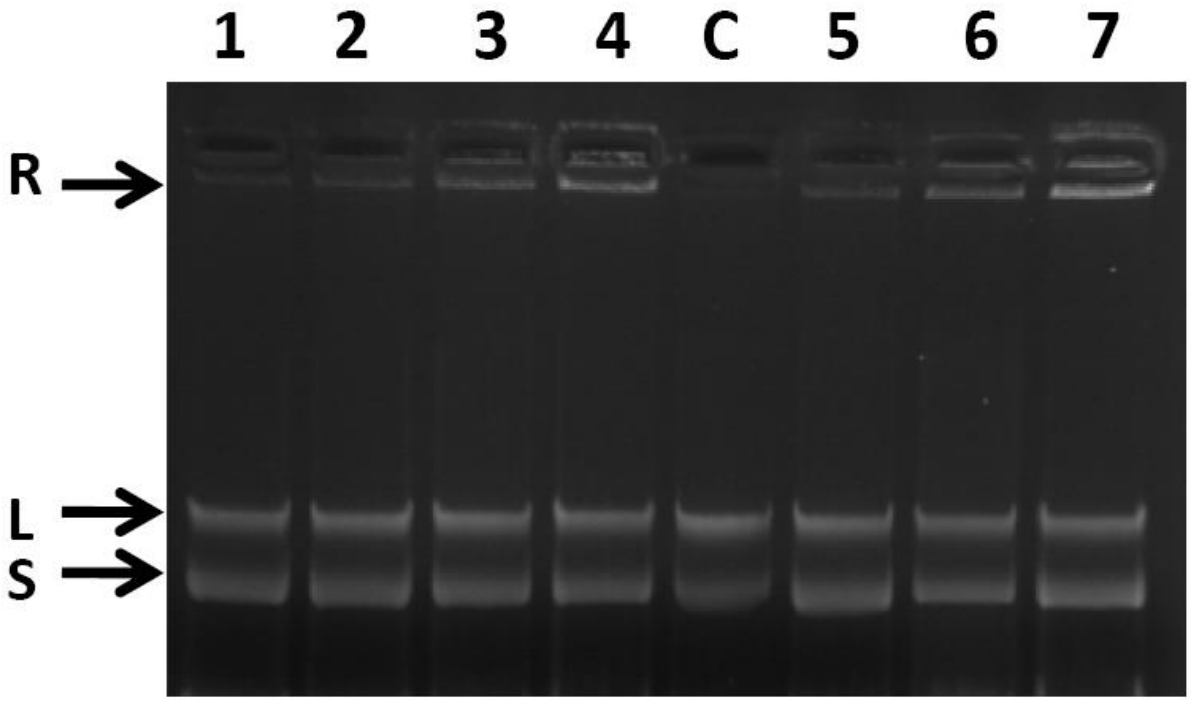

Figure 3

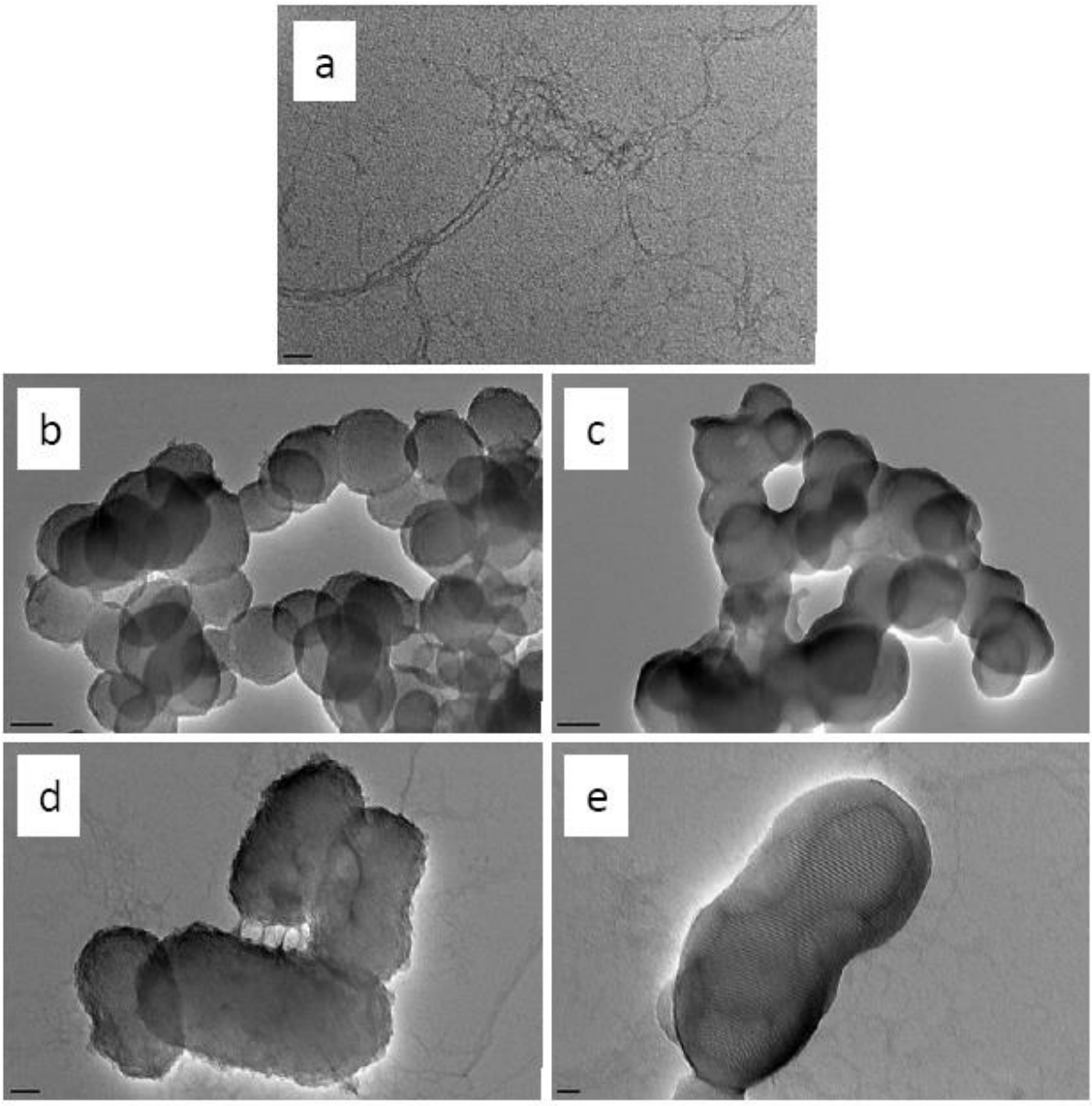

Figure 4A

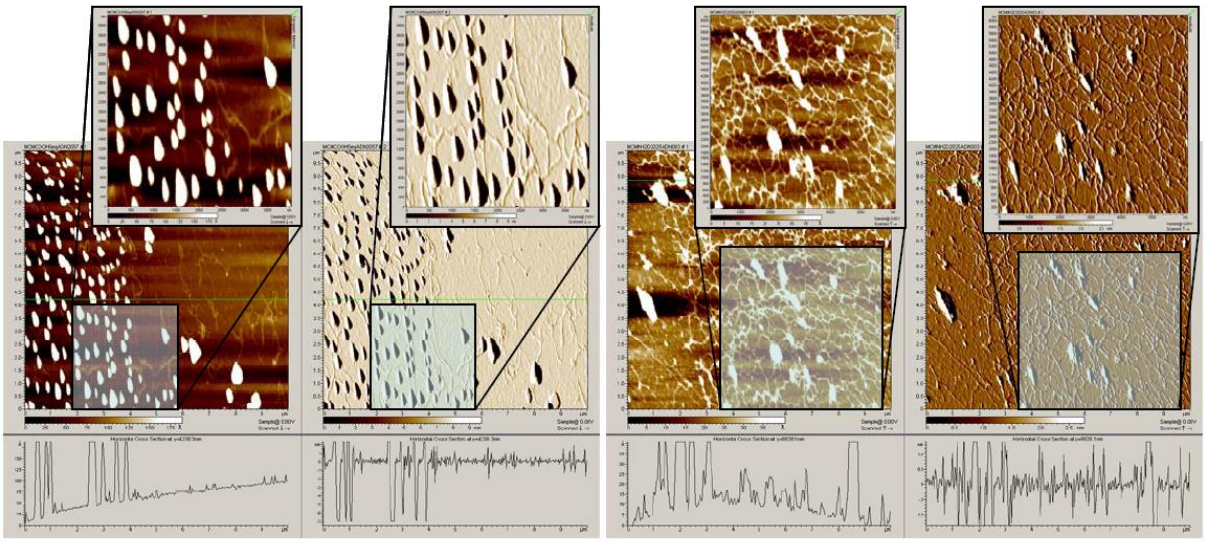

Figure 4B

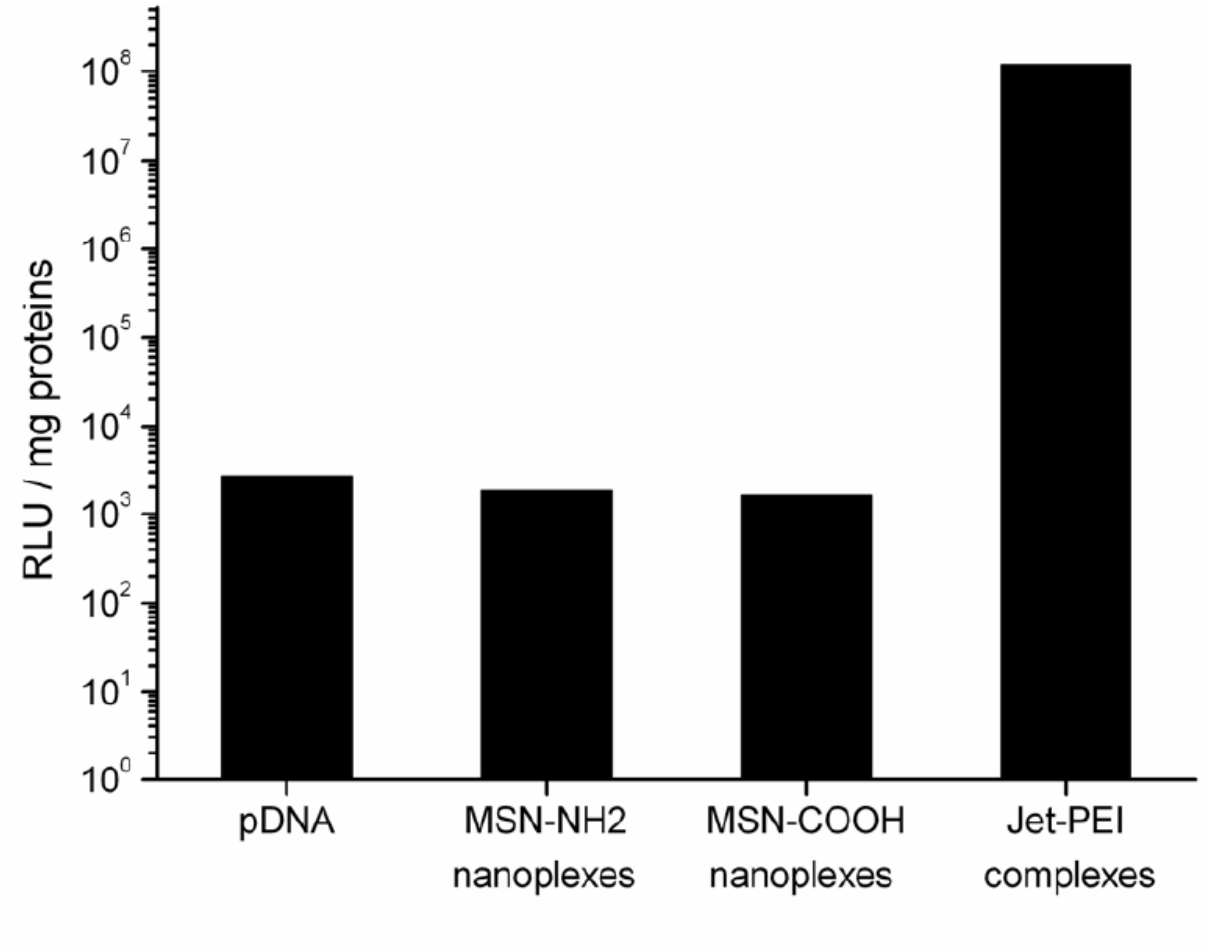
RLU / mg proteins
10^8
10^7
10^6
10^5
10^4
10^3
10^2
10^1
10^0
pDNA
MSN-NH2 nanoplexes
MSN-COOH nanoplexes
Jet-PEI complexes

Figure 5

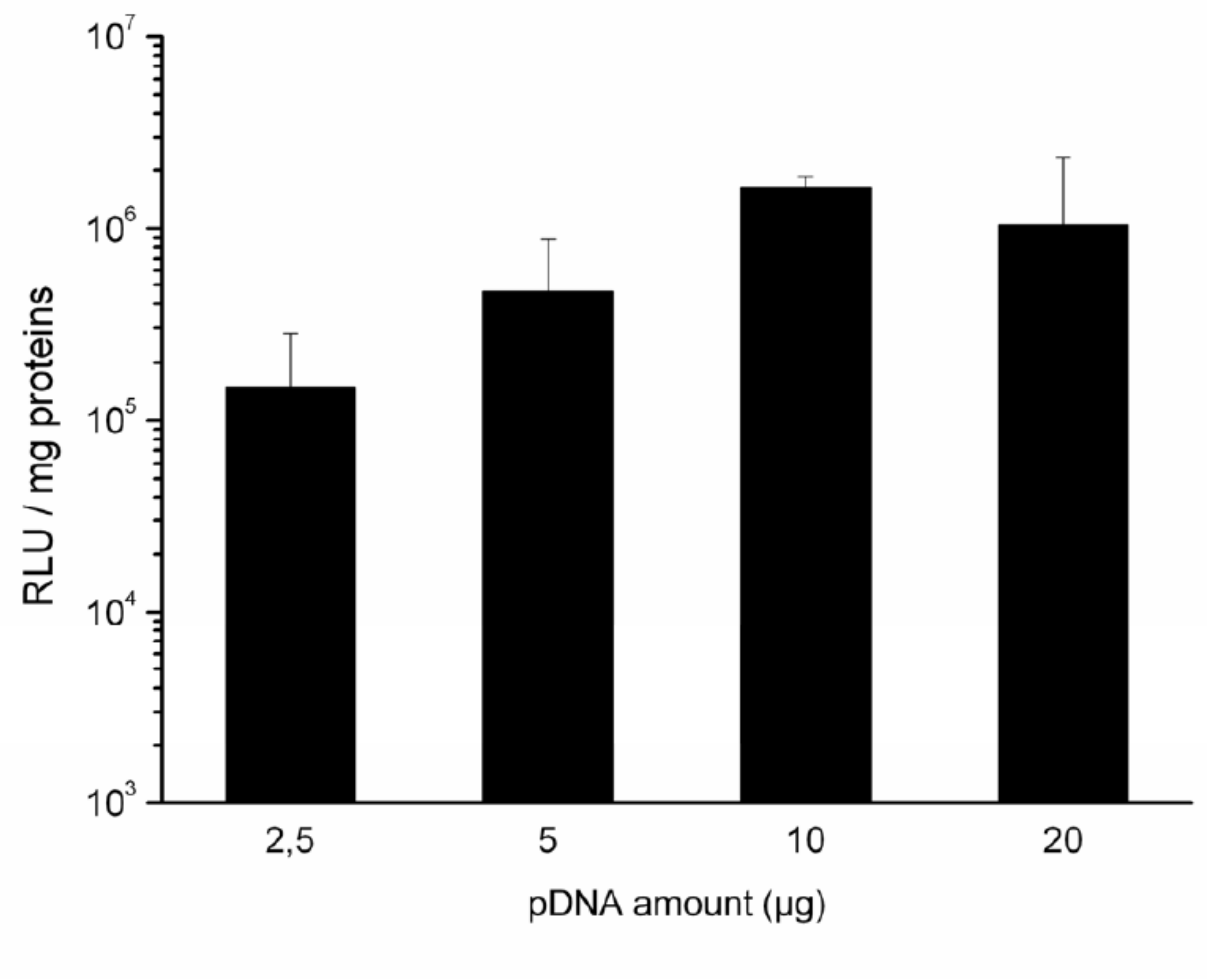

Figure 6

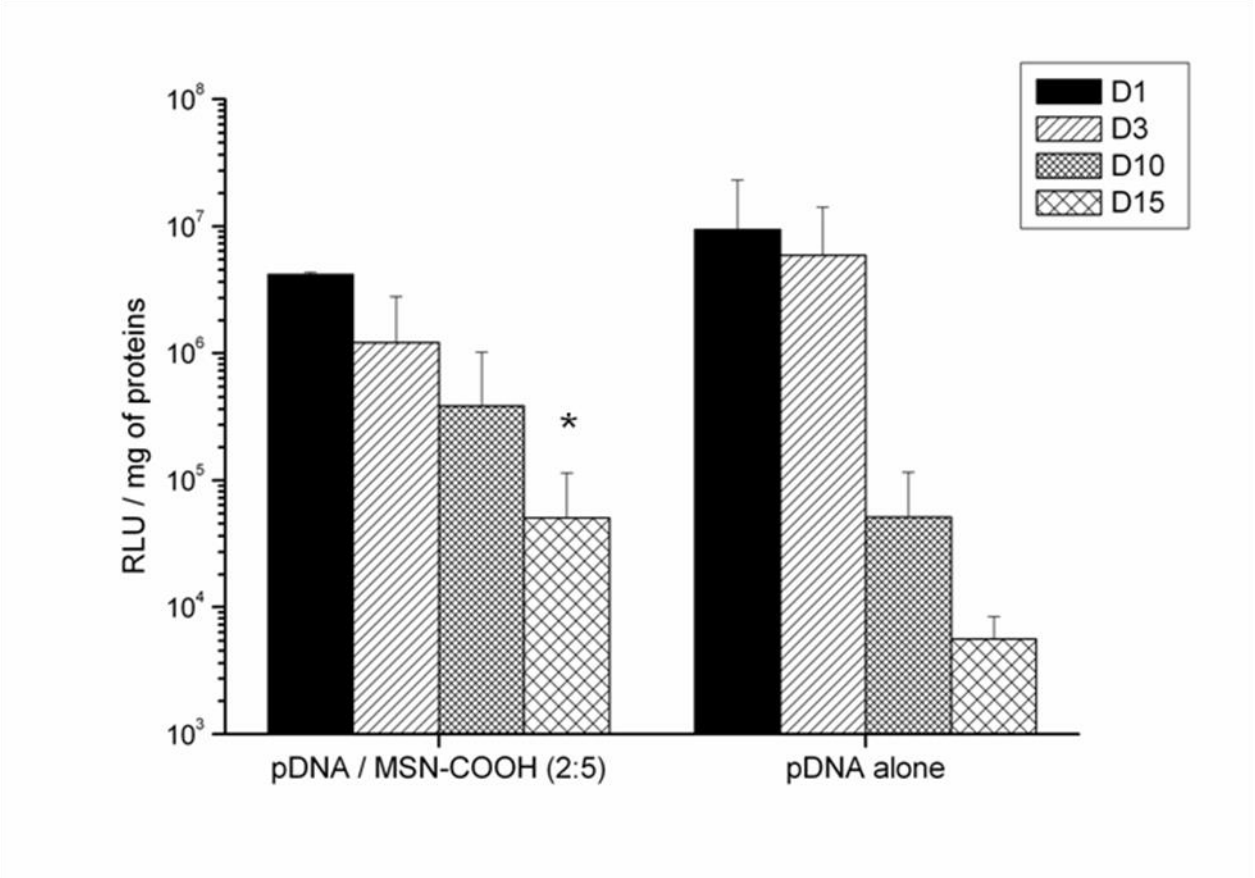
D1
D3
D10
D15
RLU / mg of proteins
10^8
10^7
10^6
10^5
10^4
10^3
*
pDNA / MSN-COOH (2:5)
pDNA alone

Figure 7

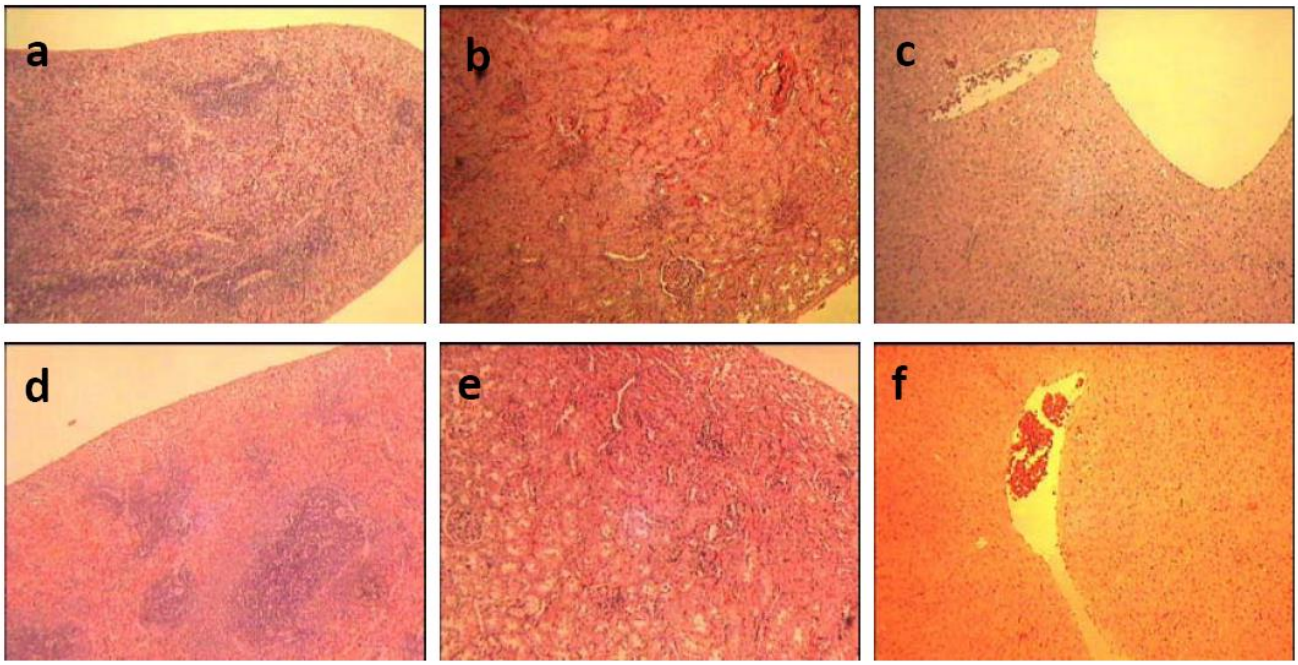

Figure 8

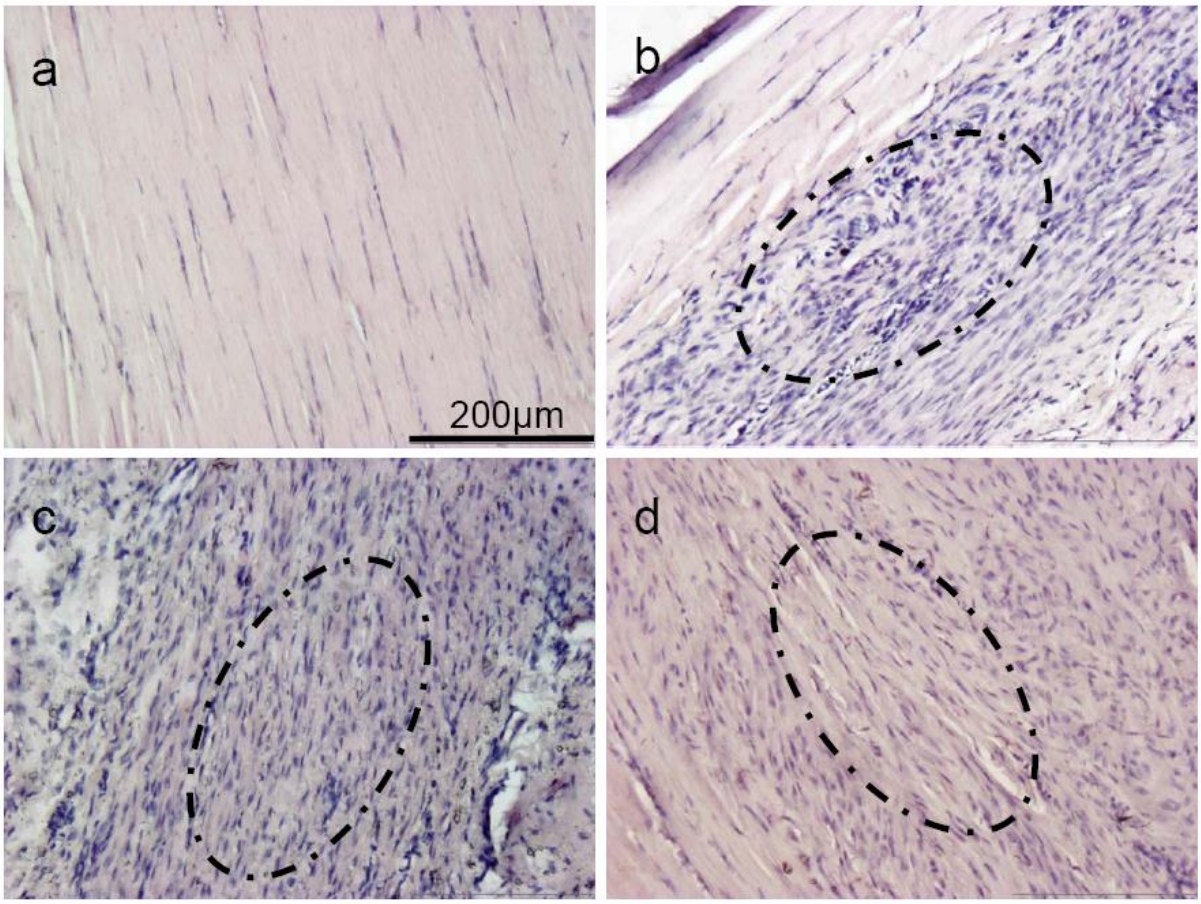

Figure 9